Prepared for submission to JHEP

Interference effects for $H \to WW/ZZ \to \ell\bar{\nu}_\ell\bar{\ell}\nu_\ell$ searches in gluon fusion at the LHC

Nikolas Kauer

Department of Physics, Royal Holloway, University of London, Egham Hill, Egham TW20 0EX, U.K.

E-mail: n.kauer@rhul.ac.uk

Abstract: WW/ZZ interference for Higgs signal and continuum background as well as signal-background interference is studied for same-flavour $\ell\bar{\nu}_\ell\bar{\ell}\nu_\ell$ final states produced in gluon-gluon scattering at the LHC for light and heavy Higgs masses with minimal and realistic experimental selection cuts. For the signal cross section, we find WW/ZZ interference effects of $\mathcal{O}(5\%)$ at $M_H = 126$ GeV. For $M_H \geq 200$ GeV, we find that WW/ZZ interference is negligible. For the gg continuum background, we also find that WW/ZZ interference is negligible. As general rule, we conclude that non-negligible WW/ZZ interference effects occur only if at least one weak boson of the pair is dominantly off-shell due to kinematic constraints. The subdominant weak boson pair contribution induces a correction to the signal-background interference, which is at the few percentage point level before search selection cuts. Optimised selection cuts for $M_H \gtrsim 600$ GeV are suggested.

Keywords: Higgs Physics, Hadron-Hadron Scattering

Contents

1 Introduction

A key objective of particle physics research is the experimental confirmation of a theoretically consistent description of elementary particle masses and electroweak symmetry breaking. The prevalent formalism is the Higgs mechanism [1–5], which predicts the existence of one or more physical Higgs bosons. Recently, a candidate Standard Model (SM) Higgs boson with $M_H \approx 126$ GeV has been discovered [6, 7]. If physics beyond the SM (BSM) is realized in nature, additional, heavier Higgs bosons may be discovered at the Large Hadron Collider (LHC). A comprehensive analysis of Higgs boson searches at the LHC can be found in refs. [8–10].

At the LHC and Tevatron, Higgs bosons are primarily produced in gluon fusion [11]. Next-to-leading order (NLO) QCD corrections have been calculated in the heavy-top limit [12] and with finite t and b mass effects [13–15], and were found to be as large as 80–100% at the LHC. This motivated the calculation of next-to-next-to-leading order (NNLO) QCD corrections [16–18] enhanced by soft-gluon resummation at next-to-next-to-leading logarithmic level [19, 20] and beyond [21]. At NNLO QCD, the residual scale uncertainty is of $\mathcal{O}(10\%)$ for inclusive observables [8]. In addition to higher-order QCD corrections, electroweak corrections have been computed and found to be at the 1–5% level [22–26].

The $H \to WW \to \ell\bar{\nu}\bar{\ell}\nu$ decay mode[1] in gluon fusion plays an important role in Higgs searches at the LHC [9, 27], and fully differential NNLO QCD [28–30] and NLO electroweak [31] corrections have been calculated and studied for this process.[2]

With inclusive NNLO signal scale uncertainties of $\mathcal{O}(10\%)$, which can be further reduced by experimental selection cuts, it is important to study signal-background interference effects, because they can be of similar size if invariant Higgs masses above the weak-boson pair threshold contribute. An accurate estimate of the magnitude of signal-background interference effects allows experimenters to decide if it has to be taken into account or may be treated as an additional uncertainty. We note that interference effects at the few percent level if neglected in SM calculations could be wrongly identified as anomalous couplings.

Higgs-continuum interference in $gg\ (\to H) \to WW$ and $gg\ (\to H) \to ZZ$ has been studied for a light and heavy SM Higgs boson in refs. [33–44]. Signal-background interference for $gg\ (\to H) \to WW \to \ell\bar{\nu}\bar{\ell}'\nu'$ (different-flavour final state) and Higgs masses between 120 GeV and 600 GeV has been analysed at LO in ref. [38] as well as refs. [36, 37, 39, 41], and including (N)NLO corrections in soft-collinear approximation in ref. [43] for $M_H = 600$ GeV. Signal-background interference for $gg\ (\to H) \to ZZ \to \ell\bar{\ell}\nu'\bar{\nu}'$ has been investigated in ref. [41] for $M_H = 125$ GeV and $M_H = 200$ GeV.

For the same-flavour final state $\ell\bar{\nu}_\ell\bar{\ell}\nu_\ell$ considered here, in addition to Higgs-continuum interference one also has interference between WW and ZZ intermediate states. The $H \to WW/ZZ \to \ell\bar{\nu}_\ell\bar{\ell}\nu_\ell$ decay including interference was calculated at LO and NLO in ref. [9, 10, 31] and interference-induced deviations of 10% for the shape of distributions have been found.[3] For continuum production, the WW/ZZ interference has been studied in $q\bar{q}$ scattering at LO in ref. [46]. No sizeable effects were found. Here, we investigate both types of interference for the gluon scattering subprocess at loop-induced LO.

The paper is organised as follows: In section 2, calculational details are discussed. WW/ZZ and signal-background interference is studied for the gluon-induced continuum background as well as light and heavy Higgs boson signals with minimal and realistic experimental selection cuts in section 3. Conclusions are given in section 4.

2 Calculational details

We implement the $gg\ (\to H) \to WW/ZZ \to \ell\bar{\nu}_\ell\bar{\ell}\nu_\ell$ process (same-flavour final state) in the publicly available parton-level program and event generator gg2VV [47], thus completing the implemention of all $gg\ (\to H) \to 4$ leptons processes at loop-induced leading order (LO).

[1] Charged leptons are denoted by ℓ.

[2] A comprehensive NLO QCD analysis of the irreducible WW+0,1 jet background including squared quark-loop contributions has been performed in ref. [32].

[3] We note that substantial interference effects between direct and indirect Higgs boson decays to quarkonia have been identified in ref. [45].

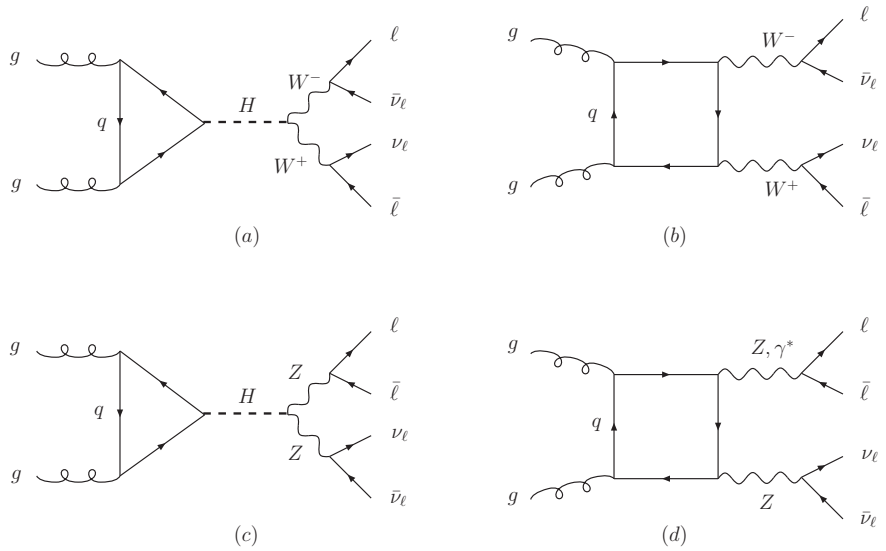

Figure 1. Representative Feynman graphs for the LO amplitude of $gg \to WW \to \ell\bar{\nu}_\ell\bar{\ell}\nu_\ell$ (Higgs signal (a) and continuum background (b) contributions) and $gg \to ZZ \to \ell\bar{\nu}_\ell\bar{\ell}\nu_\ell$ (Higgs signal (c) and continuum background (d) contributions).

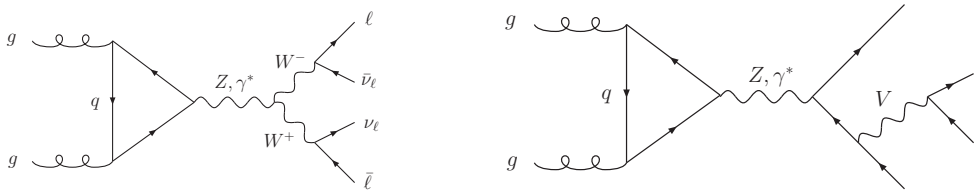

Figure 2. Representative triangle graphs that formally contribute to $gg \to \ell\bar{\nu}_\ell\bar{\ell}\nu_\ell$.

2.1 Amplitude

Figure 1 displays representative graphs for the Higgs signal process (a,c) and the gg-initiated continuum background process (b,d). For the same-flavour final state, WW intermediate states (a,b) and ZZ intermediate states (c,d) contribute. Note that the amplitude contributions (a), (b), (c) and (d) interfere. $\gamma^* \to \ell\bar{\ell}$ contributions are important for Higgs (invariant) masses below the Z-pair threshold [48] and are therefore included. In addition to box topologies, in principle also triangle topologies contribute to the gg continuum process (see figure 2). But, in the limit of vanishing lepton masses the triangle graphs do not contribute.[4]

The implementation of the amplitudes for signal and background processes is generated with FeynArts/FormCalc [49, 50] and subsequently customised. The Higgs amplitudes are implemented using the complex-pole scheme described in ref. [51]. The gg continuum am-

[4]Note that the $gg \to Z^*$ triangle graphs do contribute for non-zero lepton masses, which was verified by explicit calculation.

plitude receives contributions from box graphs that are affected by numerical instabilities when Gram determinants approach zero. In these critical phase space regions the amplitude is evaluated in quadruple precision. Residual instabilities are eliminated by requiring that $p_{T,W}$ and $p_{T,Z}$ are larger than 1 GeV.

2.2 Phase space

We use a modified version of the adaptive-importance-sampling-oriented phase space integration method employed in ref. [46] for the same-flavour $ZZ \to \ell\bar{\ell}\ell\bar{\ell}$ decay mode. Note that for a given final state, amplitudes with two distinct, potentially resonant intermediate states related via permutation contribute to the decay: $(Z \to \ell_1\bar{\ell}_1, Z \to \ell_2\bar{\ell}_2)$ and $(Z \to \ell_1\bar{\ell}_2, Z \to \ell_2\bar{\ell}_1)$. For the different-flavour case, efficient importance sampling can be achieved by applying a mapping that approximates the Breit-Wigner resonance as well as the γ^*-induced divergence at zero virtuality when integrating over both (physically distinct) Z boson virtualities $s_i = p_i^2$, where p_i is the 4-momentum of the intermediate Z boson state and $i = 1, 2$ is the flavour index. To efficiently sample the same-flavour final state, ref. [46] uses an appropriately weighted sum of the two phase space integrals corresponding to the two lepton permutations $(\bar{\ell}_1 \leftrightarrow \bar{\ell}_2)$. The phase-space-configuration-dependent weight for each channel is chosen such that not efficiently sampled resonant configurations are suppressed. Proper normalisation is achieved by overall multiplication with the inverse sum of the weights.[5] When adapting the method to $(Z \to \ell\bar{\ell}, Z \to \nu_\ell\bar{\nu}_\ell)$ and $(W \to \ell\bar{\nu}_\ell, W \to \bar{\ell}\nu_\ell)$ an asymmetry is introduced, and to preserve efficiency it is necessary to numerically balance both weight factors. This can be achieved by using

$$f_{ZZ} = \left\{\left[(s_{12} - M_W^2)^2 + (M_W\Gamma_W)^2\right] \times \left[(s_{34} - M_W^2)^2 + (M_W\Gamma_W)^2\right]\right\}^2 , \tag{2.1}$$

$$f_{WW} = \frac{s_{13}^3}{M_Z^6}\left[(s_{13} - M_Z^2)^2 + (M_Z\Gamma_Z)^2\right]^2 \times \frac{s_{24}^3}{M_Z^6}\left[(s_{24} - M_Z^2)^2 + (M_Z\Gamma_Z)^2\right]^2 , \tag{2.2}$$

with 4-momentum indices $1 = \ell$, $2 = \bar{\nu}_\ell$, $3 = \bar{\ell}$, $4 = \nu_\ell$. The integrated cross section is computed using normalised weight factors:

$$\sigma = \int_{WW} \frac{f_{WW}}{f_{WW} + f_{ZZ}}\, d\sigma + \int_{ZZ} \frac{f_{ZZ}}{f_{WW} + f_{ZZ}}\, d\sigma , \tag{2.3}$$

where the integral subscript indicates which phase space mapping is applied.

Adaptive Monte Carlo integration was carried out using the Dvegas package [52], which was developed in the context of refs. [53, 54]. The correctness of the program was checked with cross section and squared amplitude level comparisons with GoSam [55], MCFM [38, 56, 57] and VBFNLO [58, 59].

3 Results

In this section, we present cross sections and measures for interference and off-shell effects for the $gg \to \ell\bar{\nu}_\ell\bar{\ell}\nu_\ell$ process in pp collisions at $\sqrt{s} = 8$ TeV. The complete loop-induced

[5] As noted in ref. [46], in the $ZZ \to \ell\bar{\ell}\ell\bar{\ell}$ case it is advisable to randomly permute the identical leptons if final state criteria (e.g. selection cuts) are applied.

LO amplitude is included, i.e. Higgs signal and continuum background contributions as well as WW and $Z(Z,\gamma^*)$ intermediate states (collectively denoted by VV). All results are given for a single lepton flavour combination. No flavour summation is carried out for charged leptons or neutrinos.[6] As input parameters, we use the specification of the LHC Higgs Cross Section Working Group in App. A of ref. [8] with NLO weak boson widths and G_μ scheme. Finite top and bottom quark mass effects are included. Lepton masses are neglected. The fixed-width prescription is used for weak boson propagators. The complex-pole-scheme Higgs widths are calculated with the program HTO (G. Passarino, unpublished). We consider the Higgs masses 126 GeV, 200 GeV, 400 GeV, 600 GeV, 800 GeV and 1 TeV with $\Gamma_H = 4.17116$ MeV, 1.42120 GeV, 26.5977 GeV, 103.933 GeV, 235.571 GeV and 416.119 GeV, respectively. The PDF set MSTW2008 NNLO [60] with 3-loop running for $\alpha_s(\mu^2)$ and $\alpha_s(M_Z^2) = 0.11707$ is used. The CKM matrix is set to the unit matrix, which causes a negligible error [39]. Unless otherwise noted, the renormalisation and factorisation scales are fixed at $\mu_R = \mu_F = \mu_H = M_H/2$, which yields a better perturbative convergence for the signal than $\mu_R = \mu_F = M_H$ [17]. In section 3.2, the dynamic scale choice $\mu_R = \mu_F = \mu_{\text{offshell}} = M_{\ell\bar{\nu}_\ell\bar{\ell}\nu_\ell}/2$ is employed for comparison. This choice was proposed in ref. [44] for the far-off-shell region, $M_{\ell\bar{\nu}_\ell\bar{\ell}\nu_\ell} > 2M_Z$, which gives a significant contribution to the total cross section [41]. We note that at Higgs resonance, one has $\mu_H \approx \mu_{\text{offshell}}$. When a full NLO calculation of the interference becomes available, the optimal scale choice should be investigated in more detail.[7] When considering the continuum background only (section 3.1), the fixed scale $\mu_R = \mu_F = (M_W + M_Z)/2$ is used.

The resonant process $gg \to H \to \ell\bar{\nu}_\ell\bar{\ell}\nu_\ell$ (amplitude $\mathcal{M}_H$) and continuum process $gg \to \ell\bar{\nu}_\ell\bar{\ell}\nu_\ell$ (amplitude $\mathcal{M}_{\text{cont}}$) have the same initial and final states. The amplitudes therefore interfere. Furthermore, amplitude contributions with W^-W^+ and ZZ intermediate states interfere. By choosing suitable lepton flavour combinations, the W^-W^+ and ZZ contributions can be separated. Both are therefore gauge invariant. We denote the amplitudes corresponding to the graph sets (a), (b), (c) and (d) of figure 1 with $\mathcal{M}_{H,WW}$, $\mathcal{M}_{\text{cont},WW}$, $\mathcal{M}_{H,ZZ}$ and $\mathcal{M}_{\text{cont},ZZ}$, respectively. The interference is given by

$$I_{ij} = 2\,\text{Re}(\mathcal{M}_i\mathcal{M}_j^*) = |\mathcal{M}_i + \mathcal{M}_j|^2 - \rho_i - \rho_j\,, \tag{3.1}$$

where $\rho_{i,j} = |\mathcal{M}_{i,j}|^2$. As suggestive relative, symmetric, non-negative interference measure, we consider

$$R(i,j) = \frac{\sigma(\rho_i + \rho_j + I_{ij})}{\sigma(\rho_i + \rho_j)}\,, \tag{3.2}$$

and apply it to Higgs signal and continuum background contributions ($i = H$, $j = \text{cont}$)

[6] Since our study focuses on interference effects, we do not include final states with different neutrino flavours, which cannot be distinguished experimentally. Results for the corresponding different-flavour final states have been presented in ref. [41] and can be computed with gg2VV.

[7] (N)NLO corrections to signal-background interference in $gg\ (\to H) \to WW \to \ell\bar{\nu}\bar{\ell}'\nu'$ have been calculated in soft-collinear approximation in ref. [43].

as well as contributions from WW and ZZ intermediate states ($i = WW$, $j = ZZ$):

$$R_1 = R(H, \text{cont})\,, \tag{3.3}$$

$$R_3 = R(WW, ZZ)\,. \tag{3.4}$$

The contributions are described in section 2.1. When two interfering amplitude contributions are not viewed on an equal footing, the interference as relative correction to the primary contribution is a suggestive asymmetric measure:

$$\widetilde{R}(i,j) = \frac{\sigma(\rho_i + I_{ij})}{\sigma(\rho_i)}\,. \tag{3.5}$$

Employing this definition, a Higgs-boson-search-inspired alternative to R_1 is given by

$$R_2 = \widetilde{R}(H, \text{cont})\,. \tag{3.6}$$

It measures the relative signal modification due to signal-background interference, because the null hypothesis, i.e. the SM without Higgs, is not sensitive to the interference. In addition to R_3 given in eq. (3.4), we also compute the WW/ZZ interference as relative correction to the cross section of the dominant intermediate weak boson state, either WW or ZZ depending on the applied (search) selection cuts:

$$R_4 = \widetilde{R}(WW, ZZ) \qquad \text{and} \qquad R_5 = \widetilde{R}(ZZ, WW)\,, \tag{3.7}$$

respectively. Finally, for comparison the relative correction of the gluon-induced cross section due to the subdominant intermediate weak boson state is given when interference is neglected:

$$R_6 = \sigma(\rho_{ZZ})/\sigma(\rho_{WW}) \qquad \text{and} \qquad R_7 = \sigma(\rho_{WW})/\sigma(\rho_{ZZ})\,, \tag{3.8}$$

respectively.[8]

3.1 Gluon-induced continuum background

First, we consider WW/ZZ interference in the SM without Higgs boson. Continuum weak-boson pair production in gluon scattering [33, 34, 36, 38, 48, 57, 61–64] formally contributes to $pp \to \ell\bar{\nu}_\ell\bar{\ell}\nu_\ell$ at NNLO,[9] but is enhanced by the large gluon-gluon flux at the LHC (and is further enhanced by Higgs search selection cuts [63]).[10] We note that WW/ZZ interference in continuum production in quark-antiquark scattering was calculated at LO in ref. [46] and found to be negligible. Here, results for the gluon-induced continuum process $gg \to \ell\bar{\nu}_\ell\bar{\ell}\nu_\ell$ are presented in table 1. In addition to a minimal $M_{\ell\bar{\ell}} > 4$ GeV cut, we also consider LHC standard cuts for WW production ($p_{T\ell} > 20$ GeV, $|\eta_\ell| < 2.5$, $\not{p}_T > 45$ GeV, $M_{\ell\bar{\ell}} > 12$ GeV, $|M_{\ell\bar{\ell}} - M_Z| > 15$ GeV) and ZZ production ($p_{T\ell} > 20$ GeV, $|\eta_\ell| < 2.5$, $|M_{\ell\bar{\ell}} - M_Z| < 15$ GeV) [72, 73]. The renormalisation and factorisation scales are set to $(M_W + M_Z)/2$. The results demonstrate that WW/ZZ interference effects

[8] Note that due to additional contributions from undetectable non-interfering neutrino flavour combinations the phenomenological corrections are $3R_6$ and $R_7/3$.

[9] We note that electroweak corrections to $pp \to VV$ have been computed in refs. [65–67] and threshold-resummed and approximate NNLO results for $pp \to WW$ in ref. [68].

[10] We further note that cross sections for gluon-induced VV+jet production have been calculated in refs. [42, 69–71].

	$gg \to WW/ZZ \to \ell\bar{\nu}_\ell\bar{\ell}\nu_\ell$, σ [fb], pp, $\sqrt{s} = 8$ TeV			interference		correction
cuts	WW	ZZ	WW/ZZ	R_3	$R_{4/5}$	$R_{6/7}$
minimal	18.780(5)	2.4581(6)	21.241(4)	1.0001(3)	1.0002(4)	0.13089(5)
standard WW	6.243(2)	0.03914(2)	6.285(2)	1.0003(4)	1.0003(4)	0.006270(3)
standard ZZ	2.3815(7)	1.5267(4)	3.9116(8)	1.0009(3)	1.0023(8)	1.5599(6)

Table 1. Cross sections for $gg \to WW/ZZ \to \ell\bar{\nu}_\ell\bar{\ell}\nu_\ell$ in pp collisions at $\sqrt{s} = 8$ TeV for three sets of selection cuts calculated at loop-induced leading order. The interference measures $R_3 = \sigma(|\mathcal{M}_{WW} + \mathcal{M}_{ZZ}|^2)/\sigma(|\mathcal{M}_{WW}|^2 + |\mathcal{M}_{ZZ}|^2)$, $R_4 = \sigma(|\mathcal{M}_{WW}|^2 + 2\,\mathrm{Re}(\mathcal{M}_{WW}\mathcal{M}^*_{ZZ}))/\sigma(|\mathcal{M}_{WW}|^2)$ and $R_5 = \sigma(|\mathcal{M}_{ZZ}|^2 + 2\,\mathrm{Re}(\mathcal{M}_{WW}\mathcal{M}^*_{ZZ}))/\sigma(|\mathcal{M}_{ZZ}|^2)$ as well as the correction measures $R_6 = \sigma(|\mathcal{M}_{ZZ}|^2)/\sigma(|\mathcal{M}_{WW}|^2)$ and $R_7 = \sigma(|\mathcal{M}_{WW}|^2)/\sigma(|\mathcal{M}_{ZZ}|^2)$ are also displayed. $R_{4/5} = R_4$ (R_5) and $R_{6/7} = R_6$ (R_7) for minimal and standard WW cuts (standard ZZ cuts). Minimal cuts: $M_{\ell\bar{\ell}} > 4$ GeV. WW standard cuts: $p_{T\ell} > 20$ GeV, $|\eta_\ell| < 2.5$, $\not{p}_T > 45$ GeV, $M_{\ell\bar{\ell}} > 12$ GeV and $|M_{\ell\bar{\ell}} - M_Z| > 15$ GeV. ZZ standard cuts: $p_{T\ell} > 20$ GeV, $|\eta_\ell| < 2.5$, $|M_{\ell\bar{\ell}} - M_Z| < 15$ GeV. γ^* contributions are included in ZZ. Cross sections are given for a single lepton flavour combination. The integration error is displayed in brackets.

in gluon-fusion continuum production are negligible. Table 1 also demonstrates that the ZZ correction to WW production is of $\mathcal{O}(10\%)$ with minimal selection cuts, but becomes negligible when standard WW selection cuts are applied. In contrast, the WW correction to ZZ production is of $\mathcal{O}(1)$ when standard ZZ selection cuts are applied.

3.2 Light Higgs boson signal

We now study signal-background and WW/ZZ interference effects in the Standard Model with a 126 GeV Higgs boson motivated by the recent discovery [6, 7]. Results for minimal, standard and Higgs search cuts are shown in tables 2, 4 and 5, respectively. As above, a minimal $M_{\ell\bar{\ell}} > 4$ GeV cut is applied to exclude the on-shell photon singularity. In this section, we apply the following cuts as standard cuts for the $WW \to \ell\bar{\nu}_\ell\bar{\ell}\nu_\ell$ process at the LHC:[11] $p_{T\ell,1\mathrm{st}} > 25$ GeV, $p_{T\ell,2\mathrm{nd}} > 15$ GeV, $|\eta_\ell| < 2.5$, $\not{p}_T > 45$ GeV, $M_{\ell\bar{\ell}} > 12$ GeV and $|M_{\ell\bar{\ell}} - M_Z| > 15$ GeV. As $H \to WW$ search cuts, we apply these standard cuts and in addition $M_{\ell\bar{\ell}} < 50$ GeV, $\Delta\phi_{\ell\bar{\ell}} < 1.8$ and $0.75\,M_H < M_T < M_H$ [72].[12] The cut on the transverse mass

$$M_{T1} = \sqrt{(M_{T,\ell\bar{\ell}} + \not{p}_T)^2 - (\mathbf{p}_{T,\ell\bar{\ell}} + \not{\mathbf{p}}_T)^2} \quad \text{with} \quad M_{T,\ell\bar{\ell}} = \sqrt{p^2_{T,\ell\bar{\ell}} + M^2_{\ell\bar{\ell}}} \tag{3.9}$$

strongly reduces the contribution from $M_{\ell\bar{\nu}_\ell\bar{\ell}\nu_\ell} > M_H$ [38].[13] The renormalisation and factorisation scales are set to $\mu_R = \mu_F = M_H/2$, except in table 3.

For the Higgs signal cross section, we find negative WW/ZZ interference of approximately 5%, whereas no significant WW/ZZ interference occurs for the continuum background in agreement with our findings in section 3.1. This difference can be traced back

[11] The staggered $p_{T\ell}$ cut accomodates the off-shell W boson decay for $M_{WW} \approx 126$ GeV. Leptons are ordered by decreasing p_T.

[12] Very similar selection cuts are employed in ref. [73].

[13] In the absence of additional final state particles, the expression for M_{T1} simplifies due to $\not{\mathbf{p}}_T = -\mathbf{p}_{T,\ell\ell}$.

	$gg\ (\to H) \to VV \to \ell\bar{\nu}_\ell\bar{\ell}\nu_\ell$, σ [fb], pp, $\sqrt{s} = 8$ TeV, $M_H = 126$ GeV, min. cuts			interference	
VV	H	cont	$\lvert H{+}\text{cont}\rvert^2$	R_1	R_2
WW	17.593(4)	20.978(5)	36.480(8)	0.9458(3)	0.8811(6)
ZZ	0.9308(3)	2.7543(7)	3.436(2)	0.9324(5)	0.732(2)
WW/ZZ	17.729(3)	23.742(5)	39.125(8)	0.9434(3)	0.8677(6)
R_3	0.9571(3)	1.0004(3)	0.9802(3)		
R_4	0.9548(3)	1.0004(4)	0.9783(3)		
R_6	0.05291(2)	0.13129(5)	0.09419(5)		

Table 2. Cross sections and interference measures for $gg\ (\to H) \to WW/ZZ \to \ell\bar{\nu}_\ell\bar{\ell}\nu_\ell$ in pp collisions at $\sqrt{s} = 8$ TeV. The off-shell Higgs cross section at $M_H = 126$ GeV, the gluon-induced continuum cross section and the sum including interference are given. The signal-background interference measures $R_1 = \sigma(|\mathcal{M}_H + \mathcal{M}_{\text{cont}}|^2)/\sigma(|\mathcal{M}_H|^2 + |\mathcal{M}_{\text{cont}}|^2)$ and $R_2 = \sigma(|\mathcal{M}_H|^2 + 2\,\text{Re}(\mathcal{M}_H\mathcal{M}^*_{\text{cont}}))/\sigma(|\mathcal{M}_H|^2)$ as well as several WW/ZZ-related interference and correction measures (see table 1) are also displayed. A minimal $M_{\ell\bar{\ell}} > 4$ GeV cut is applied. Other details as in table 1.

	$gg\ (\to H) \to VV \to \ell\bar{\nu}_\ell\bar{\ell}\nu_\ell$, σ [fb], pp, $\sqrt{s} = 8$ TeV, $M_H = 126$ GeV, min. cuts, $\mu_R = \mu_F = M_{\ell\bar{\nu}_\ell\bar{\ell}\nu_\ell}/2$			interference	
VV	H	cont	$\lvert H{+}\text{cont}\rvert^2$	R_1	R_2
WW	17.318(4)	16.925(4)	32.803(8)	0.9580(3)	0.9169(6)
ZZ	0.8822(2)	2.1553(6)	2.872(1)	0.9455(4)	0.813(2)
WW/ZZ	17.402(3)	19.084(4)	34.884(7)	0.9561(3)	0.9079(5)
R_3	0.9562(3)	1.0002(3)	0.9778(3)		
R_4	0.9540(3)	1.0002(4)	0.9759(4)		
R_6	0.05094(2)	0.12735(5)	0.08756(4)		

Table 3. Cross sections and interference measures for $gg\ (\to H) \to WW/ZZ \to \ell\bar{\nu}_\ell\bar{\ell}\nu_\ell$ in pp collisions at $\sqrt{s} = 8$ TeV and $M_H = 126$ GeV. The dynamic scale $\mu_R = \mu_F = M_{\ell\bar{\nu}_\ell\bar{\ell}\nu_\ell}/2$ is employed. Details as in table 2.

to the fact that for $H \to VV$ with $M_V < M_H < 2M_V$ the most likely configuration features one weak boson (W as well as Z) that is (far) off-shell, whereas for the continuum background no such kinematic constraint exists.

Signal-background interference effects for minimal, standard and Higgs search cuts are compatible with what would be expected on the basis of different-flavour final state results [38, 41]. With minimal and standard cuts, the signal-background interference of the subdominant ZZ contribution when measured with R_2 is significantly larger than for the dominant WW contribution. Due to the suppression of the ZZ contribution (high with standard and search cuts), the induced change of the overall signal-background interference

	$gg\ (\to H) \to VV \to \ell\bar{\nu}_\ell\bar{\ell}\nu_\ell$, σ [fb], pp, $\sqrt{s} = 8$ TeV, $M_H = 126$ GeV, std. cuts			interference	
VV	H	cont	$\lvert H+\text{cont}\rvert^2$	R_1	R_2
WW	3.606(2)	8.084(3)	10.442(3)	0.8932(3)	0.654(1)
ZZ	0.009752(6)	0.05099(3)	0.05387(3)	0.8868(7)	0.295(5)
WW/ZZ	3.545(3)	8.17(2)	10.46(2)	0.893(3)	0.646(8)
R_3	0.9804(8)	1.004(3)	0.996(2)		
R_4	0.9803(8)	1.004(3)	0.996(2)		
R_6	0.002704(2)	0.006308(5)	0.005159(4)		

Table 4. Cross sections and interference measures for $gg\ (\to H) \to WW/ZZ \to \ell\bar{\nu}_\ell\bar{\ell}\nu_\ell$ in pp collisions at $\sqrt{s} = 8$ TeV and $M_H = 126$ GeV. WW standard cuts for $M_{WW} \approx 126$ GeV are applied: $p_{T\ell,1\text{st}} > 25$ GeV, $p_{T\ell,2\text{nd}} > 15$ GeV, $|\eta_\ell| < 2.5$, $\not{p}_T > 45$ GeV, $M_{\ell\bar{\ell}} > 12$ GeV and $|M_{\ell\bar{\ell}} - M_Z| > 15$ GeV. Other details as in table 2.

	$gg\ (\to H) \to VV \to \ell\bar{\nu}_\ell\bar{\ell}\nu_\ell$, σ [fb], pp, $\sqrt{s} = 8$ TeV, $M_H = 126$ GeV, Higgs search cuts			interference	
VV	H	cont	$\lvert H+\text{cont}\rvert^2$	R_1	R_2
WW	2.9303(7)	0.7836(4)	3.6649(8)	0.9868(4)	0.9833(4)
ZZ	0.004658(3)	0.002851(2)	0.007494(3)	0.9979(6)	0.9966(9)
WW/ZZ	2.8758(7)	0.7864(4)	3.6131(8)	0.9866(3)	0.9829(4)
R_3	0.9799(4)	0.9999(8)	0.9839(3)		
R_4	0.9798(4)	0.9999(8)	0.9838(3)		
R_6	0.0015898(9)	0.003638(3)	0.002045(1)		

Table 5. Cross sections and interference measures for $gg\ (\to H) \to WW/ZZ \to \ell\bar{\nu}_\ell\bar{\ell}\nu_\ell$ in pp collisions at $\sqrt{s} = 8$ TeV and $M_H = 126$ GeV. Higgs search cuts are applied, i.e. WW standard cuts (as in table 4) and $M_{\ell\bar{\ell}} < 50$ GeV, $\Delta\phi_{\ell\bar{\ell}} < 1.8$ and $0.75\, M_H < M_{T1} < M_H$. The transverse mass M_{T1} is defined in eq. (3.9) in the main text. Other details as in table 2.

is, however, at most at the one-percentage-point level. As seen in table 5, the application of a $M_{T1} < M_H$ cut suppresses the interference effects even stronger for the ZZ contribution than for the WW contribution.

Results for $\mu_R = \mu_F = M_{\ell\bar{\nu}_\ell\bar{\ell}\nu_\ell}/2$ and minimal cut are displayed in table 3. Signal-background interference effects are smaller compared to $\mu_R = \mu_F = M_H/2$, because the dynamic scale reduces the contribution of the region with strong interference, due to the smaller strong coupling at higher VV invariant mass. R_2 decreases by 3–8 percentage points relative to table 2. Changes in the WW/ZZ interference measures are at the sub-percentage point level.

3.3 Heavy Higgs boson signal

We now study the signal-background and WW/ZZ interference in the same-flavour decay mode for a SM-like Higgs boson with mass between 200 GeV and 1 TeV. A priori, the search for a SM Higgs boson in the intermediate and heavy mass range is a crucial task. It continues without premature conclusion about the exact nature of the discovered boson at 126 GeV. More specifically, one can search for a heavier SM Higgs boson with the advantage that assumptions about the realized SM extension are not required. Given that the discovered 126 GeV boson appears to have all characteristics of the SM Higgs boson, an alternative, slightly better motivated approach is to search for a second, heavier Higgs boson. A first proposal for a framework for the interpretation of the continuing LHC Higgs searches at masses other than 126 GeV has been set out in ref. [10]. These searches are being conducted in a model-independent way by suitably rescaling SM predictions in order to preserve unitarity cancellations at high energies as well as by considering specific BSM benchmark models. It is straightforward to apply the rescaling procedure described in ref. [10] to the results presented in this section. We note that the program gg2VV can be used to study Higgs-continuum interference and off-shell effects for BSM scenarios with a SM-like Higgs boson with rescaled Hgg, HWW and HZZ couplings. The analysis of BSM benchmark models is beyond the scope of this paper.

In this context, the question arises if Higgs-Higgs interference effects are small. The SM-like Higgs boson at 126 GeV appears to have the expected tiny width of approx. 4 MeV.[14] The overlap of the extremely narrow Breit-Wigner lineshape with the lineshape of a heavier Higgs boson with experimentally discriminable mass is insignificant. Higgs-Higgs interference effects are thus expected to be negligible provided that off-shell effects [41, 83] are suppressed by the search selection cuts.[15]

Both approaches, a heavy SM or BSM Higgs boson search at the LHC (denoted by "SM" and "BSM" below), have been pursued by ATLAS and CMS for Higgs masses up to 1 TeV. In the following, we quote the experimental exclusion limits for a heavy Higgs boson with SM properties. The $H \to ZZ \to \ell\bar{\ell}\ell\bar{\ell}$ (same or different flavour) and $H \to ZZ \to \ell\bar{\ell}\nu\bar{\nu}$ channels yield the strongest limits.[16] The four-charged-lepton channel has been studied by ATLAS (SM) [85] and CMS (SM) [86]. An exclusion region of 130–827 GeV is given in the latter work. Secondly, the $H \to ZZ \to \ell\bar{\ell}\nu\bar{\nu}$ channel has been studied by CMS (SM and BSM) [87] and ATLAS (SM, $M_H < 600$ GeV, 7 TeV data) [88]. CMS and ATLAS exclude a mass in the ranges 248–930 GeV and 319–558 GeV, respectively. Furthermore, the $H \to WW \to \ell\bar{\nu}\bar{\ell}\nu$ channel has been analysed by ATLAS (SM) [89] and CMS (SM) [90], excluding the mass ranges 260–642 GeV and 128-600 GeV, respectively. The semileptonic decay modes $H \to WW \to \ell\nu jj$ [91, 92] and $H \to ZZ \to \ell\bar{\ell}jj$ [93] have also been studied by ATLAS (SM) and CMS (SM and BSM). A combined analysis of $H \to ZZ$ and $H \to WW$ channels in the mass range 145 GeV to 1 TeV has been carried out by CMS [94] and an update is in preparation [95].

[14] Bounding Γ_H at $M_H \approx 126$ GeV with LHC and Tevatron data has been studied in refs. [44, 74–82].

[15] We note that the role of interference effects in analysing the tensor structure of the HZZ coupling has been studied in ref. [84].

[16] All exclusion limits are given at 95% confidence level.

		$gg\ (\to H) \to VV \to \ell\bar{\nu}_\ell\bar{\ell}\nu_\ell$, σ [fb], pp, $\sqrt{s} = 8$ TeV, minimal cut			interference		
M_H [GeV]	VV	H	cont	$\lvert H{+}\text{cont}\rvert^2$	R_1	R_2	H/cont
200	WW	23.662(7)	17.781(5)	41.677(9)	1.0057(3)	1.0099(5)	1.3307(6)
	ZZ	3.125(1)	2.327(2)	5.565(2)	1.0208(4)	1.0363(7)	1.3431(8)
	WW/ZZ	26.781(7)	20.114(5)	47.242(9)	1.0074(3)	1.0129(5)	1.3315(5)
	R_3	0.9998(4)	1.0003(4)	1.0000(3)			
	R_4	0.9998(4)	1.0003(4)	1.0000(3)			
	R_6	0.13208(6)	0.13086(8)	0.13354(5)			
400	WW	8.548(3)	14.078(4)	22.405(5)	0.9902(3)	0.9742(8)	0.6072(3)
	ZZ	1.5053(7)	1.8298(7)	3.318(1)	0.9948(4)	0.9886(9)	0.8226(5)
	WW/ZZ	10.053(3)	15.912(4)	25.727(5)	0.9908(3)	0.9764(7)	0.6318(3)
	R_3	1.0000(5)	1.0002(4)	1.0002(3)			
	R_4	1.0000(5)	1.0003(4)	1.0002(3)			
	R_6	0.1761(1)	0.12998(6)	0.14809(5)			
600	WW	1.430(3)	12.354(4)	14.142(5)	1.0260(5)	1.250(5)	0.1157(2)
	ZZ	0.2600(4)	1.6014(7)	1.9016(8)	1.0216(6)	1.154(5)	0.1624(3)
	WW/ZZ	1.690(3)	13.959(4)	16.047(5)	1.0255(4)	1.236(4)	0.1211(2)
	R_3	1.000(2)	1.0003(4)	1.0002(4)			
	R_4	1.000(3)	1.0003(5)	1.0003(5)			
	R_6	0.1819(4)	0.12963(7)	0.13447(7)			
800	WW	0.2857(7)	11.286(3)	11.806(3)	1.0202(4)	1.82(2)	0.02531(6)
	ZZ	0.0527(2)	1.4602(6)	1.5425(6)	1.0195(6)	1.56(2)	0.03611(8)
	WW/ZZ	0.3384(7)	12.750(3)	13.352(3)	1.0201(4)	1.78(2)	0.02654(6)
	R_3	1.000(3)	1.0003(4)	1.0003(4)			
	R_4	1.000(4)	1.0003(4)	1.0003(4)			
	R_6	0.1845(6)	0.12938(6)	0.13065(6)			
1000	WW	0.0759(4)	10.547(3)	10.760(3)	1.0129(4)	2.81(6)	0.00720(3)
	ZZ	0.01409(4)	1.3616(6)	1.3939(6)	1.0132(6)	2.29(6)	0.01034(3)
	WW/ZZ	0.0900(4)	11.911(3)	12.157(3)	1.0129(4)	2.73(5)	0.00755(3)
	R_3	1.000(5)	1.0003(4)	1.0003(4)			
	R_4	1.000(6)	1.0003(4)	1.0003(4)			
	R_6	0.1856(9)	0.12910(7)	0.12955(7)			

Table 6. Cross sections and interference measures for $gg\ (\to H) \to WW/ZZ \to \ell\bar{\nu}_\ell\bar{\ell}\nu_\ell$ in pp collisions at $\sqrt{s} = 8$ TeV with a Higgs boson mass in the range 200 GeV to 1 TeV. A minimal $M_{\ell\bar{\ell}} > 4$ GeV cut is applied. Other details as in table 2.

3.3.1 Minimal cuts

As in section 3.2, the renormalisation and factorisation scales are set to $\mu_R = \mu_F = M_H/2$. Again, we first give results for a minimal $M_{\ell\bar{\ell}} > 4$ GeV cut. To cover the heavy Higgs mass range of interest, results are shown in table 6 for a Higgs mass of 200 GeV, 400 GeV, 600

M_H [GeV]	200	400	600	800	1000
M_{T2} lower bound [GeV]	180	300	420	500	550
M_{T2} upper bound [GeV]	220	450	700	900	1100
$\not{p}_T$ lower bound [GeV]	20	90	110	150	170

Table 7. Higgs-mass-dependent $H \to ZZ$ search cuts. Bounding cuts are applied to the transverse mass M_{T2} defined in eq. (3.10) in the main text and the missing transverse momentum $\not{p}_T$.

GeV, 800 GeV and 1 TeV.

In contrast to the light Higgs case, we find that WW/ZZ interference for the Higgs signal is negligible for all considered heavy Higgs masses. This further supports our conclusion in section 3.2, which is that non-negligible WW/ZZ interference effects occur only if at least one weak boson of the pair is dominantly off-shell due to kinematic constraints. This assertion is also confirmed by the results given in sections 3.3.2 and 3.3.3, where heavy Higgs search selection cuts are applied. With minimal cut the ZZ correction is of $\mathcal{O}(10$–$20\%)$ and effects a change of the signal-background interference at the few percentage-point level. For Higgs masses beyond 700 GeV, signal-over-background ratios are at the percent and per mil level, and signal-background interference $(R_2 - 1)$ is of $\mathcal{O}(1)$.

3.3.2 $H \to ZZ$ search cuts

While the four-charged-lepton channel has the highest sensitivity in the $H \to ZZ$ search for masses below 500 GeV, the $H \to ZZ \to \ell\bar{\ell}\nu\bar{\nu}$ channel considered here dominates above 500 GeV [95]. As above, we consider the Higgs mass range 200 GeV–1 TeV and note that for the lower end of this range the $H \to WW \to \ell\bar{\ell}\nu\bar{\nu}$ process can contribute as much as 70% to the signal after selection cuts [88]. For our calculations, we adopt the analysis strategy of the recent study presented in ref. [87]. In more detail, as $H \to ZZ$ search cuts we apply the basic selection cuts $p_{T\ell} > 20$ GeV, $|\eta_\ell| < 2.5$ and $|M_{\ell\bar{\ell}} - M_Z| < 15$ GeV. In addition, to select the signal contribution with $M_{ZZ} \approx M_H$ Higgs-mass-dependent bounds are imposed on the transverse mass M_{T2} and $\not{p}_T$.[17] M_{T2} is given by

$$M_{T2} = \sqrt{\left(M_{T,\ell\bar{\ell}} + \not{M}_T\right)^2 - (\mathbf{p}_{T,\ell\bar{\ell}} + \not{\mathbf{p}}_T)^2} \quad \text{with} \quad \not{M}_T = \sqrt{\not{p}_T^2 + M_{\ell\bar{\ell}}^2}\,. \tag{3.10}$$

$M_{T,\ell\bar{\ell}}$ is defined in eq. (3.9).[18] The employed M_{T2} and $\not{p}_T$ bounds are given in table 7. Note that an upper bound is imposed on M_{T2} for all Higgs masses in order to suppress increasingly large interference effects at high invariant masses.

Applying these $H \to ZZ$ search cuts, we obtain the results shown in table 8, which demonstrate the absence of WW/ZZ interference for the Higgs signal and continuum background. Signal-background interference $(R_2 - 1)$ ranges from -2% to $+60\%$ and is not affected by the WW correction for $M_H \gtrsim 400$ GeV.

[17] In our calculation, $p_{T,\ell\bar{\ell}}$ is constrained by the $\not{p}_T$ cut.

[18] In the absence of additional final state particles: $M_{T2} = 2M_{T,\ell\bar{\ell}} = 2\not{M}_T$.

		$gg\ (\to H) \to VV \to \ell\bar{\ell}\nu_\ell\bar{\nu}_\ell$, σ [fb], pp, $\sqrt{s} = 8$ TeV, $H \to ZZ$ cuts			interference		
M_H [GeV]	VV	H	cont	$\lvert H+\text{cont}\rvert^2$	R_1	R_2	H/cont
200	ZZ	1.7507(5)	0.6224(3)	2.5153(6)	1.0600(4)	1.0813(5)	2.813(2)
	WW	2.2529(9)	1.0064(6)	3.338(2)	1.0243(5)	1.0351(7)	2.239(2)
	ZZ/WW	3.997(1)	1.6302(6)	5.848(2)	1.0392(3)	1.0552(5)	2.452(2)
	R_3	0.9983(4)	1.0009(6)	0.9990(3)			
	R_5	0.9961(8)	1.002(2)	0.9976(7)			
	R_7	1.2869(6)	1.617(2)	1.3272(6)			
400	ZZ	0.8919(3)	0.07674(7)	0.9508(3)	0.9816(5)	0.9800(5)	11.62(1)
	WW	0.02340(2)	0.01400(3)	0.03909(4)	1.045(2)	1.073(2)	1.672(4)
	ZZ/WW	0.9154(3)	0.09074(7)	0.9901(3)	0.9840(4)	0.9824(5)	10.088(9)
	R_3	1.0001(5)	1.000(2)	1.0001(5)			
	R_5	1.0001(5)	1.000(2)	1.0001(5)			
	R_7	0.02623(2)	0.1824(4)	0.04111(4)			
600	ZZ	0.15889(9)	0.02187(1)	0.18949(9)	1.0483(7)	1.0549(8)	7.263(5)
	$WW/10^{-4}$	0.232(2)	1.57(3)	1.98(4)	1.10(3)	1.8(2)	0.148(3)
	ZZ/WW	0.15891(9)	0.02204(1)	0.18970(9)	1.0484(7)	1.0551(8)	7.211(5)
	R_3	1.0000(8)	1.0002(7)	1.0001(7)			
	R_5	1.0000(8)	1.0002(7)	1.0001(7)			
	R_7	0.000146(2)	0.0072(2)	0.00105(2)			
800	ZZ	0.03191(2)	0.010964(4)	0.05113(2)	1.1928(6)	1.2590(8)	2.910(2)
	$WW/10^{-5}$	0.069(3)	2.91(9)	3.1(1)	1.04(5)	3(2)	0.024(2)
	ZZ/WW	0.03191(2)	0.010994(4)	0.05117(2)	1.1927(6)	1.2591(8)	2.902(2)
	R_3	1.0000(7)	1.0001(6)	1.0000(5)			
	R_5	1.0000(7)	1.0001(6)	1.0000(5)			
	R_7	$2.2(1)\cdot10^{-5}$	0.00265(9)	0.00061(2)			
1000	ZZ	0.008415(3)	0.007268(2)	0.020719(6)	1.3211(5)	1.5984(9)	1.1578(5)
	$WW/10^{-5}$	0.0086(4)	1.22(5)	1.25(5)	1.02(6)	4(8)	0.0071(5)
	ZZ/WW	0.008416(3)	0.007281(2)	0.020733(6)	1.3208(5)	1.5984(9)	1.1558(5)
	R_3	1.0000(5)	1.0001(4)	1.0000(4)			
	R_5	1.0000(5)	1.0001(4)	1.0000(4)			
	R_7	0.00001(1)	0.00168(7)	0.00060(3)			

Table 8. Cross sections and interference measures for $gg\ (\to H) \to ZZ/WW \to \ell\bar{\ell}\nu_\ell\bar{\nu}_\ell$ in pp collisions at $\sqrt{s} = 8$ TeV with a Higgs boson mass in the range 200 GeV to 1 TeV. $H \to ZZ$ search cuts are applied: $p_{T\ell} > 20$ GeV, $|\eta_\ell| < 2.5$, $|M_{\ell\bar{\ell}} - M_Z| < 15$ GeV and the M_H-dependent cuts displayed in table 7. Other details as in table 2.

3.3.3 $H \to WW$ search cuts

We adopt the $H \to WW$ search cuts of ref. [90].[19] To simulate detector coverage, select $WW \to \ell\bar{\nu}\bar{\ell}\nu$ and suppress reducible backgrounds the following cuts are applied: $|\eta_\ell| < 2.5$, $\not{p}_T > 20$ GeV, $M_{\ell\bar{\ell}} > 12$ GeV, $|M_{\ell\bar{\ell}} - M_Z| > 15$ GeV and $p_{T,\ell\bar{\ell}} > 45$ GeV. To select the $H \to WW$ signal, following ref. [90], we define the transverse mass

$$M_{T3} = \sqrt{2\, p_{T,\ell\bar{\ell}}\, \not{p}_T (1 - \cos\Delta\phi_{\ell\bar{\ell},\text{miss}})}\,, \tag{3.11}$$

where $\Delta\phi_{\ell\bar{\ell},\text{miss}}$ is the angle between $\mathbf{p}_{T,\ell\bar{\ell}}$ and $\not{\mathbf{p}}_T$, and impose the cuts $p_{T\ell,\text{max}} > 0.2\, M_H$, $p_{T\ell,\text{min}} > 25$ GeV, $M_{\ell\bar{\ell}} < 90$ GeV for $M_H = 200$ GeV and $M_{\ell\bar{\ell}} < M_H - 100$ GeV for $M_H \geq 400$ GeV, $\Delta\phi_{\ell\bar{\ell}} < 100^\circ$ for $M_H = 200$ GeV and $\Delta\phi_{\ell\bar{\ell}} < 175^\circ$ for $M_H \geq 400$ GeV, and 120 GeV $< M_{T3} < M_H$.[20]

With these $H \to WW$ search cuts, we obtain the results shown in table 9. The cuts reduce the ZZ correction to the one-percent level, and the signal-background interference is dominated by the WW contribution.

4 Conclusions

We studied WW/ZZ interference for Higgs signal and continuum background as well as signal-background interference for same-flavour $\ell\bar{\nu}_\ell\bar{\ell}\nu_\ell$ final states produced in gluon-gluon scattering at the LHC for light and heavy Higgs masses with minimal and realistic experimental selection cuts. For the signal cross section, we find WW/ZZ interference effects of $\mathcal{O}(5\%)$ at $M_H = 126$ GeV. For $M_H \geq 200$ GeV, we find that WW/ZZ interference is negligible. For the gg continuum background, we also find that WW/ZZ interference is negligible. As general rule, we conclude that non-negligible WW/ZZ interference effects occur only if at least one weak boson of the pair is dominantly off-shell due to kinematic constraints. Our results demonstrate that in cases where WW/ZZ interference can be neglected it is nevertheless important to take into account the subdominant weak boson pair as its contribution is of $\mathcal{O}(10\text{–}20\%)$ before search selection cuts are applied. Considering WW intermediate states in $H \to ZZ$ searches is crucial due to the intrinsically larger continuum cross section. The subdominant weak boson pair contribution induces a correction to the signal-background interference, which is at the few percentage point level except when selection cuts strongly suppress the subdominant contribution. To mitigate the signal reduction in heavy Higgs searches due to increasingly large negative signal-background interference for invariant masses above the Higgs mass, we employed an upper bound cut on the transverse mass also for $M_H \gtrsim 600$ GeV. The kinematical dependence of signal-background and WW/ZZ interference for $gg \to H \to WW/ZZ \to \ell\bar{\nu}_\ell\bar{\ell}\nu_\ell$ can be calculated and simulated with the public parton-level event generator gg2VV.

[19] In ref. [89] the same-lepton-flavour final states have not been included.

[20] In the absence of additional final state particles: $M_{T3} = 2\, p_{T,\ell\bar{\ell}} = 2\, \not{p}_T$.

		$gg\ (\to H) \to VV \to \ell\bar{\nu}_\ell\bar{\ell}\nu_\ell$, σ [fb], pp, $\sqrt{s} = 8$ TeV, $H \to WW$ cuts			interference		
M_H [GeV]	VV	H	cont	$\lvert H+\text{cont}\rvert^2$	R_1	R_2	H/cont
200	WW	3.686(2)	1.5060(8)	5.614(2)	1.0812(4)	1.1144(6)	2.448(2)
	ZZ	0.008678(7)	0.003983(3)	0.012141(8)	0.9589(8)	0.940(2)	2.179(3)
	WW/ZZ	3.701(2)	1.5100(8)	5.633(2)	1.0809(4)	1.1139(6)	2.451(2)
	R_3	1.0017(5)	1.0000(7)	1.0012(4)			
	R_4	1.0017(5)	1.0000(7)	1.0012(4)			
	R_6	0.002354(2)	0.002645(3)	0.002163(2)			
400	WW	2.5009(9)	0.6197(3)	2.9806(9)	0.9551(4)	0.9440(5)	4.036(3)
	ZZ	0.03929(3)	0.00983(2)	0.04896(4)	0.997(1)	0.996(2)	3.995(9)
	WW/ZZ	2.5401(9)	0.6298(4)	3.0297(9)	0.9558(4)	0.9448(5)	4.033(3)
	R_3	1.0000(5)	1.0004(7)	1.0000(5)			
	R_4	1.0000(5)	1.0004(7)	1.0000(5)			
	R_6	0.01571(2)	0.01587(4)	0.01643(2)			
600	WW	0.5260(3)	0.2659(2)	0.8386(4)	1.0590(6)	1.0888(9)	1.978(2)
	ZZ	0.006632(5)	0.00347(2)	0.01099(2)	1.087(3)	1.133(4)	1.909(8)
	WW/ZZ	0.5326(3)	0.2694(2)	0.8496(4)	1.0593(6)	1.0893(9)	1.977(2)
	R_3	1.0000(7)	1.0002(7)	1.0000(6)			
	R_4	1.0000(7)	1.0002(7)	1.0000(6)			
	R_6	0.01261(2)	0.01306(6)	0.01310(3)			
800	WW	0.10346(5)	0.10562(5)	0.23894(9)	1.1428(6)	1.289(2)	0.9795(7)
	ZZ	0.0012318(8)	0.001252(9)	0.00291(1)	1.173(6)	1.35(2)	0.984(7)
	WW/ZZ	0.10469(5)	0.10689(5)	0.24185(9)	1.1431(6)	1.289(2)	0.9794(7)
	R_3	1.0000(7)	1.0001(7)	1.0000(6)			
	R_4	1.0000(7)	1.0001(7)	1.0000(6)			
	R_6	0.01191(1)	0.01186(9)	0.01219(4)			
1000	WW	0.02426(2)	0.04357(2)	0.08049(3)	1.1867(6)	1.522(2)	0.5568(4)
	ZZ	0.0002958(2)	0.000512(4)	0.000986(4)	1.220(7)	1.60(2)	0.577(4)
	WW/ZZ	0.02455(2)	0.04408(2)	0.08148(3)	1.1871(6)	1.523(2)	0.5570(4)
	R_3	1.0000(7)	1.0001(7)	1.0000(6)			
	R_4	1.0000(7)	1.0001(7)	1.0000(6)			
	R_6	0.01219(1)	0.01176(8)	0.01225(5)			

Table 9. Cross sections and interference measures for $gg\ (\to H) \to WW/ZZ \to \ell\bar{\nu}_\ell\bar{\ell}\nu_\ell$ in pp collisions at $\sqrt{s} = 8$ TeV with a Higgs boson mass in the range 200 GeV to 1 TeV. $H \to WW$ search cuts are applied: $p_{T\ell,\text{max}} > 0.2\,M_H$, $p_{T\ell,\text{min}} > 25$ GeV, $|\eta_\ell| < 2.5$, $\not{p}_T > 20$ GeV, $p_{T,\ell\bar{\ell}} > 45$ GeV, $M_{\ell\bar{\ell}} > 12$ GeV, $|M_{\ell\bar{\ell}} - M_Z| > 15$ GeV, $M_{\ell\bar{\ell}} < 90$ GeV for $M_H = 200$ GeV and $M_{\ell\bar{\ell}} < M_H - 100$ GeV for $M_H \geq 400$ GeV, $\Delta\phi_{\ell\bar{\ell}} < 100°$ for $M_H = 200$ GeV and $\Delta\phi_{\ell\bar{\ell}} < 175°$ for $M_H \geq 400$ GeV, 120 GeV $< M_{T3} < M_H$. The transverse mass M_{T3} is defined in eq. (3.11) in the main text. Other details as in table 2.

Acknowledgments

I would like to thank the conveners and members of the LHC Higgs Cross Section Working Group, notably S. Bolognesi, D. de Florian, S. Diglio, C. Mariotti, G. Passarino and R. Tanaka, for stimulating and informative discussions, G. Heinrich, M. Rauch and M. Rodgers for useful comparisons, and the Centre for Particle Physics at Royal Holloway, University of London and the Institute for Theoretical Particle Physics and Cosmology at RWTH Aachen University for access to their computing facilities. Financial support from the Higher Education Funding Council for England, the Science and Technology Facilities Council and the Institute for Particle Physics Phenomenology, Durham, is gratefully acknowledged.

References

[1] P. W. Higgs, *Broken symmetries, massless particles and gauge fields*, Phys. Lett. **12** (1964) 132.

[2] P. W. Higgs, *Broken symmetries and the masses of gauge bosons*, Phys. Rev. Lett. **13** (1964) 508.

[3] P. W. Higgs, *Spontaneous symmetry breakdown without massless bosons*, Phys. Rev. **145** (1966) 1156.

[4] F. Englert and R. Brout, *Broken symmetry and the mass of gauge vector mesons*, Phys. Rev. Lett. **13** (1964) 321.

[5] G. S. Guralnik, C. R. Hagen and T. W. B. Kibble, *Global conservation laws and massless particles*, Phys. Rev. Lett. **13** (1964) 585.

[6] G. Aad *et al.* [ATLAS Collaboration], *Observation of a new particle in the search for the Standard Model Higgs boson with the ATLAS detector at the LHC*, Phys. Lett. B **716** (2012) 1 [arXiv:1207.7214 [hep-ex]].

[7] S. Chatrchyan *et al.* [CMS Collaboration], *Observation of a new boson at a mass of 125 GeV with the CMS experiment at the LHC*, Phys. Lett. B **716** (2012) 30 [arXiv:1207.7235 [hep-ex]].

[8] S. Dittmaier *et al.*, *Handbook of LHC Higgs cross sections: 1. Inclusive observables*, arXiv:1101.0593 [hep-ph].

[9] S. Dittmaier *et al.*, *Handbook of LHC Higgs cross sections: 2. Differential distributions*, arXiv:1201.3084 [hep-ph].

[10] S. Heinemeyer *et al.*, *Handbook of LHC Higgs cross sections: 3. Higgs properties*, arXiv:1307.1347 [hep-ph].

[11] H. M. Georgi, S. L. Glashow, M. E. Machacek and D. V. Nanopoulos, *Higgs bosons from two-gluon annihilation in proton-proton collisions*, Phys. Rev. Lett. **40** (1978) 692.

[12] S. Dawson, *Radiative corrections to Higgs boson production*, Nucl. Phys. B **359** (1991) 283.

[13] A. Djouadi, M. Spira and P. M. Zerwas, *Production of Higgs bosons in proton colliders: QCD corrections*, Phys. Lett. B **264** (1991) 440.

[14] D. Graudenz, M. Spira and P. M. Zerwas, *QCD corrections to Higgs boson production at proton-proton colliders*, Phys. Rev. Lett. **70** (1993) 1372.

[15] M. Spira, A. Djouadi, D. Graudenz and P. M. Zerwas, *Higgs boson production at the LHC*, Nucl. Phys. B **453** (1995) 17 [hep-ph/9504378].

[16] R. V. Harlander and W. B. Kilgore, *Next-to-next-to-leading order Higgs production at hadron colliders*, Phys. Rev. Lett. **88** (2002) 201801 [hep-ph/0201206].

[17] C. Anastasiou and K. Melnikov, *Higgs boson production at hadron colliders in NNLO QCD*, Nucl. Phys. B **646** (2002) 220 [arXiv:hep-ph/0207004].

[18] V. Ravindran, J. Smith and W. L. van Neerven, *NNLO corrections to the total cross section for Higgs boson production in hadron-hadron collisions*, Nucl. Phys. B **665** (2003) 325 [arXiv:hep-ph/0302135].

[19] S. Catani, D. de Florian, M. Grazzini and P. Nason, *Soft-gluon resummation for Higgs boson production at hadron colliders*, JHEP **0307** (2003) 028 [hep-ph/0306211].

[20] D. de Florian, G. Ferrera, M. Grazzini and D. Tommasini, *Transverse-momentum resummation: Higgs boson production at the Tevatron and the LHC*, JHEP **1111** (2011) 064 [arXiv:1109.2109 [hep-ph]].

[21] S. Moch and A. Vogt, *Higher-order soft corrections to lepton pair and Higgs boson production*, Phys. Lett. B **631** (2005) 48 [hep-ph/0508265].

[22] A. Djouadi and P. Gambino, *Leading electroweak correction to Higgs boson production at proton colliders*, Phys. Rev. Lett. **73** (1994) 2528 [hep-ph/9406432].

[23] U. Aglietti, R. Bonciani, G. Degrassi and A. Vicini, *Two-loop light fermion contribution to Higgs production and decays*, Phys. Lett. B **595** (2004) 432 [hep-ph/0404071].

[24] G. Degrassi and F. Maltoni, *Two-loop electroweak corrections to Higgs production at hadron colliders*, Phys. Lett. B **600** (2004) 255 [hep-ph/0407249].

[25] S. Actis, G. Passarino, C. Sturm and S. Uccirati, *NLO electroweak corrections to Higgs boson production at hadron colliders*, Phys. Lett. B **670** (2008) 12 [arXiv:0809.1301 [hep-ph]].

[26] C. Anastasiou, R. Boughezal and F. Petriello, *Mixed QCD-electroweak corrections to Higgs boson production in gluon fusion*, JHEP **0904** (2009) 003 [arXiv:0811.3458 [hep-ph]].

[27] M. Dittmar and H. K. Dreiner, *How to find a Higgs boson with a mass between 155 GeV – 180 GeV at the LHC*, Phys. Rev. D **55** (1997) 167 [hep-ph/9608317].

[28] C. Anastasiou, G. Dissertori and F. Stockli, *NNLO QCD predictions for the $H \to WW \to \ell\nu\ell\nu$ signal at the LHC*, JHEP **0709** (2007) 018 [arXiv:0707.2373 [hep-ph]].

[29] M. Grazzini, *NNLO predictions for the Higgs boson signal in the $H \to WW \to \ell\nu\ell\nu$ and $H \to ZZ \to 4\ell$ decay channels*, JHEP **0802** (2008) 043 [arXiv:0801.3232 [hep-ph]].

[30] C. Anastasiou, G. Dissertori, F. Stockli and B. R. Webber, *QCD radiation effects on the $H \to WW \to \ell\nu\ell\nu$ signal at the LHC*, JHEP **0803** (2008) 017 [arXiv:0801.2682 [hep-ph]].

[31] A. Bredenstein, A. Denner, S. Dittmaier and M. M. Weber, *Precise predictions for the Higgs-boson decay $H \to WW/ZZ \to 4$ leptons*, Phys. Rev. D **74** (2006) 013004 [hep-ph/0604011].

[32] F. Cascioli, S. Hoeche, F. Krauss, P. Maierhofer, S. Pozzorini and F. Siegert, *Precise Higgs-background predictions: merging NLO QCD and squared quark-loop corrections to four-lepton + 0,1 jet production*, arXiv:1309.0500 [hep-ph].

[33] E. W. N. Glover and J. J. van der Bij, *Vector boson pair production via gluon fusion*, Phys. Lett. B **219** (1989) 488.

[34] E. W. N. Glover and J. J. van der Bij, *Z-boson pair production via gluon fusion*, Nucl. Phys. B **321** (1989) 561.

[35] M. H. Seymour, *The Higgs boson line shape and perturbative unitarity*, Phys. Lett. B **354** (1995) 409 [hep-ph/9505211].

[36] T. Binoth, M. Ciccolini, N. Kauer and M. Kramer, *Gluon-induced W-boson pair production at the LHC*, JHEP **0612** (2006) 046 [hep-ph/0611170].

[37] E. Accomando, *The process $gg \to WW$ as a probe into the EWSB mechanism*, Phys. Lett. B **661** (2008) 129 [arXiv:0709.1364 [hep-ph]].

[38] J. M. Campbell, R. K. Ellis and C. Williams, *Gluon-gluon contributions to W^+W^- production and Higgs interference effects*, JHEP **1110** (2011) 005 [arXiv:1107.5569 [hep-ph]].

[39] N. Kauer, *Signal-background interference in $gg \to H \to VV$*, PoS RADCOR **2011** (2011) 027 [arXiv:1201.1667 [hep-ph]].

[40] G. Passarino, *Higgs interference effects in $gg \to ZZ$ and their uncertainty*, JHEP **1208** (2012) 146 [arXiv:1206.3824 [hep-ph]].

[41] N. Kauer and G. Passarino, *Inadequacy of zero-width approximation for a light Higgs boson signal*, JHEP **1208** (2012) 116 [arXiv:1206.4803 [hep-ph]].

[42] F. Campanario, Q. Li, M. Rauch and M. Spira, *ZZ+jet production via gluon fusion at the LHC*, JHEP **1306** (2013) 069 [arXiv:1211.5429 [hep-ph]].

[43] M. Bonvini, F. Caola, S. Forte, K. Melnikov and G. Ridolfi, *Signal-background interference effects for $gg \to H \to W^+W^-$ beyond leading order*, arXiv:1304.3053 [hep-ph].

[44] F. Caola and K. Melnikov, *Constraining the Higgs boson width with ZZ production at the LHC*, arXiv:1307.4935 [hep-ph].

[45] G. T. Bodwin, F. Petriello, S. Stoynev and M. Velasco, *Higgs boson decays to quarkonia and the $H\bar{c}c$ coupling*, arXiv:1306.5770 [hep-ph].

[46] T. Melia, P. Nason, R. Rontsch and G. Zanderighi, *W^+W^-, WZ and ZZ production in the POWHEG BOX*, JHEP **1111** (2011) 078 [arXiv:1107.5051 [hep-ph]].

[47] http://gg2VV.hepforge.org/

[48] T. Binoth, N. Kauer and P. Mertsch, *Gluon-induced QCD corrections to $pp \to ZZ \to \ell\bar{\ell}\ell'\bar{\ell}'$*, arXiv:0807.0024 [hep-ph].

[49] T. Hahn, *Generating Feynman diagrams and amplitudes with FeynArts 3*, Comput. Phys. Commun. **140** (2001) 418 [arXiv:hep-ph/0012260].

[50] T. Hahn and M. Perez-Victoria, *Automatized one-loop calculations in four and D dimensions*, Comput. Phys. Commun. **118** (1999) 153 [arXiv:hep-ph/9807565].

[51] S. Goria, G. Passarino and D. Rosco, *The Higgs boson lineshape*, Nucl. Phys. B **864** (2012) 530 [arXiv:1112.5517 [hep-ph]].

[52] http://Dvegas.hepforge.org/

[53] N. Kauer and D. Zeppenfeld, *Finite-width effects in top quark production at hadron colliders*, Phys. Rev. D **65** (2002) 014021 [hep-ph/0107181].

[54] N. Kauer, *Top-pair production beyond double pole approximation: pp, $p\bar{p} \to$ six fermions and zero, one or two additional partons*, Phys. Rev. D **67** (2003) 054013 [hep-ph/0212091].

[55] G. Cullen, N. Greiner, G. Heinrich, G. Luisoni, P. Mastrolia, G. Ossola, T. Reiter and F. Tramontano, *Automated one-loop calculations with GoSam*, Eur. Phys. J. C **72** (2012) 1889 [arXiv:1111.2034 [hep-ph]].

[56] J. M. Campbell and R. K. Ellis, *An update on vector boson pair production at hadron colliders*, Phys. Rev. D **60** (1999) 113006 [arXiv:hep-ph/9905386].

[57] J. M. Campbell, R. K. Ellis and C. Williams, *Vector boson pair production at the LHC*, JHEP **1107** (2011) 018 [arXiv:1105.0020 [hep-ph]].

[58] K. Arnold, M. Bahr, G. Bozzi, F. Campanario, C. Englert, T. Figy, N. Greiner and C. Hackstein *et al.*, *VBFNLO: a parton-level Monte Carlo for processes with electroweak bosons*, Comput. Phys. Commun. **180** (2009) 1661 [arXiv:0811.4559 [hep-ph]].

[59] K. Arnold, J. Bellm, G. Bozzi, M. Brieg, F. Campanario, C. Englert, B. Feigl and J. Frank *et al.*, *VBFNLO: a parton-level Monte Carlo for processes with electroweak bosons – manual for version 2.6.0*, arXiv:1107.4038 [hep-ph].

[60] A. D. Martin, W. J. Stirling, R. S. Thorne and G. Watt, *Parton distributions for the LHC*, Eur. Phys. J. C **63** (2009) 189 [arXiv:0901.0002 [hep-ph]].

[61] D. A. Dicus, C. Kao and W. W. Repko, *Gluon production of gauge bosons*, Phys. Rev. D **36** (1987) 1570.

[62] C. Zecher, T. Matsuura and J. J. van der Bij, *Leptonic signals from off-shell Z-boson pairs at hadron colliders*, Z. Phys. C **64** (1994) 219 [hep-ph/9404295].

[63] T. Binoth, M. Ciccolini, N. Kauer and M. Kramer, *Gluon-induced WW background to Higgs boson searches at the LHC*, JHEP **0503** (2005) 065 [hep-ph/0503094].

[64] R. Frederix, S. Frixione, V. Hirschi, F. Maltoni, R. Pittau and P. Torrielli, *Four-lepton production at hadron colliders: aMC@NLO predictions with theoretical uncertainties*, JHEP **1202** (2012) 099 [arXiv:1110.4738 [hep-ph]].

[65] A. Bierweiler, T. Kasprzik, J. H. Kuhn and S. Uccirati, *Electroweak corrections to W-boson pair production at the LHC*, JHEP **1211** (2012) 093 [arXiv:1208.3147 [hep-ph]].

[66] A. Bierweiler, T. Kasprzik and J. H. Kuhn, *Vector-boson pair production at the LHC to $\mathcal{O}(\alpha^3)$ accuracy*, arXiv:1305.5402 [hep-ph].

[67] J. Baglio, Le D. N. and M. M. Weber, *Massive gauge boson pair production at the LHC: a next-to-leading order story*, arXiv:1307.4331 [hep-ph].

[68] S. Dawson, I. M. Lewis and M. Zeng, *Threshold resummed and approximate NNLO results for W^+W^- pair production at the LHC*, Phys. Rev. D **88** (2013) 054028 [arXiv:1307.3249 [hep-ph]].

[69] T. Melia, K. Melnikov, R. Rontsch, M. Schulze and G. Zanderighi, *Gluon fusion contribution to W^+W^-+ jet production*, JHEP **1208** (2012) 115 [arXiv:1205.6987 [hep-ph]].

[70] P. Agrawal and A. Shivaji, *Di-vector boson + jet production via gluon fusion at hadron colliders*, Phys. Rev. D **86** (2012) 073013 [arXiv:1207.2927 [hep-ph]].

[71] P. Agrawal and A. Shivaji, *Production of γZg and associated processes via gluon fusion at hadron colliders*, JHEP **1301** (2013) 071 [arXiv:1208.2593 [hep-ph]].

[72] G. Aad *et al.* [ATLAS Collaboration], *Measurements of Higgs boson production and couplings in diboson final states with the ATLAS detector at the LHC*, arXiv:1307.1427 [hep-ex].

[73] S. Chatrchyan *et al.* [CMS Collaboration], *Observation of a new boson with mass near 125 GeV in pp collisions at* $\sqrt{s} = 7$ *and 8 TeV*, JHEP **06** (2013) 081 [arXiv:1303.4571 [hep-ex]].

[74] V. Barger, M. Ishida and W. Y. Keung, *Total width of 125 GeV Higgs boson*, Phys. Rev. Lett. **108** (2012) 261801 [arXiv:1203.3456 [hep-ph]].

[75] B. A. Dobrescu and J. D. Lykken, *Coupling spans of the Higgs-like boson*, JHEP **1302** (2013) 073 [arXiv:1210.3342 [hep-ph]].

[76] J. Ellis and T. You, *Updated global analysis of Higgs couplings*, JHEP **1306** (2013) 103 [arXiv:1303.3879 [hep-ph]].

[77] A. Djouadi and G. Moreau, *The couplings of the Higgs boson and its CP properties from fits of the signal strengths and their ratios at the 7+8 TeV LHC*, arXiv:1303.6591 [hep-ph].

[78] CMS Collaboration, *Combination of Standard Model Higgs boson searches and measurements of the properties of the new boson with a mass near 125 GeV*, CMS-PAS-HIG-13-005.

[79] S. P. Martin, *Shift in the LHC Higgs diphoton mass peak from interference with background*, Phys. Rev. D **86** (2012) 073016 [arXiv:1208.1533 [hep-ph]].

[80] K. Cheung, J. S. Lee and P. Y. Tseng, *Higgs precision (higgcision) era begins*, JHEP **1305** (2013) 134 [arXiv:1302.3794 [hep-ph]].

[81] L. J. Dixon and Y. Li, *Bounding the Higgs boson width through interferometry*, arXiv:1305.3854 [hep-ph].

[82] G. Belanger, B. Dumont, U. Ellwanger, J. F. Gunion and S. Kraml, *Global fit to Higgs signal strengths and couplings and implications for extended Higgs sectors*, arXiv:1306.2941 [hep-ph].

[83] N. Kauer, *Inadequacy of zero-width approximation for a light Higgs boson signal*, Mod. Phys. Lett. A **28** (2013) 1330015 [arXiv:1305.2092 [hep-ph]].

[84] M. Chen, T. Cheng, J. S. Gainer, A. Korytov, K. T. Matchev, P. Milenovic, G. Mitselmakher, M. Park, A. Rinkevicius and M. Snowball, *The role of interference in unraveling the ZZ-couplings of the newly discovered boson at the LHC*, arXiv:1310.1397 [hep-ph].

[85] ATLAS Collaboration, *Measurements of the properties of the Higgs-like boson in the four-lepton decay channel with the ATLAS detector using 25* fb^{-1} *of proton-proton collision data*, ATLAS-CONF-2013-013.

[86] CMS Collaboration, *Properties of the Higgs-like boson in the decay* $H \to ZZ \to 4\ell$ *in pp collisions at* $\sqrt{s} = 7$ *and 8 TeV*, CMS-PAS-HIG-13-002.

[87] CMS Collaboration, *Search for a heavy Higgs boson in the* $H \to ZZ \to 2\ell 2\nu$ *channel in pp collisions at* $\sqrt{s} = 7$ *and 8 TeV*, CMS-PAS-HIG-13-014.

[88] G. Aad *et al.* [ATLAS Collaboration], *Search for a Standard Model Higgs boson in the* $H \to ZZ \to \ell^+\ell^-\nu\bar{\nu}$ *decay channel using 4.7* fb^{-1} *of* $\sqrt{s} = 7$ *TeV data with the ATLAS detector*, Phys. Lett. B **717** (2012) 29 [arXiv:1205.6744 [hep-ex]].

[89] ATLAS Collaboration, *Search for a high-mass Higgs boson in the* $H \to WW \to \ell\nu\ell\nu$ *decay channel with the ATLAS detector using 21* fb^{-1} *of proton-proton collision data*, ATLAS-CONF-2013-067.

[90] CMS Collaboration, *Evidence for a particle decaying to* W^+W^- *in the fully leptonic final state in a Standard Model Higgs boson search in pp collisions at the LHC*, CMS-PAS-HIG-13-003.

[91] G. Aad *et al.* [ATLAS Collaboration], *Search for the Higgs boson in the $H \to WW \to \ell\nu jj$ decay channel at $\sqrt{s} = 7$ TeV with the ATLAS detector*, Phys. Lett. B **718** (2012) 391 [arXiv:1206.6074 [hep-ex]].

[92] CMS Collaboration, *Search for a Standard Model-like Higgs boson decaying into $WW \to \ell\nu q\bar{q}'$ in pp collisions at $\sqrt{s} = 8$ TeV*, CMS-PAS-HIG-13-008.

[93] G. Aad *et al.* [ATLAS Collaboration], *Search for a Standard Model Higgs boson in the mass range 200–600 GeV in the $H \to ZZ \to \ell^+\ell^- q\bar{q}$ decay channel with the ATLAS detector*, Phys. Lett. B **717** (2012) 70 [arXiv:1206.2443 [hep-ex]].

[94] S. Chatrchyan *et al.* [CMS Collaboration], *Search for a Standard-Model-like Higgs boson with a mass in the range 145 to 1000 GeV at the LHC*, Eur. Phys. J. C **73** (2013) 2469 [arXiv:1304.0213 [hep-ex]].

[95] J. Wang [ATLAS and CMS Collaborations], *High-mass Higgs to WW or ZZ*, Talk presented at Higgs Hunting 2013, Orsay, France, July 2013.